VIA MEDICA

ORIGINAL ARTICLE

Folia Morphol.
Vol. 79, No. 1, pp. 141–147
DOI: 10.5603/FM.a2019.0064

ISSN 0015–5659
journals.viamedica.pl

Comparison of the ossification centre images between standard computed tomography and micro-computed tomography

W. Wang[1#], X. Wang[2, 3#], X. Ren[4], L. Chen[5], Z. Li[3*], X. Li[3], P. Zhang[6], J. Gao[7], B. Su[3], S. Zhang[3*]

[1]*Department of Emergency, Inner Mongolia People's Hospital, Hohhot, China*
[2]*Institute of Traditional Chinese Medicine, Beijing University of Chinese Medicine, Beijing, China*
[3]*Human Anatomy Teaching and Research Section (Digital Medical Centre), Inner Mongolia Medical University Basic Medical College, Hohhot, China*
[4]*Department of Endocrinology, Affiliated Hospital of Inner Mongolia Medical University, Hohhot, China*
[5]*Department of Haematology, Affiliated Hospital of Inner Mongolia Medical University, Hohhot, China*
[6]*Department of Imaging Diagnosis, Affiliated Hospital of Inner Mongolia Medical University, Hohhot, China*
[7]*Medical Imaging Department, Inner Mongolia People's Hospital, Hohhot, China*

Received: 26 March 2019; Accepted: 8 May 2019]

Background: *Based on standard computed tomography (CT) and micro-CT scan axis images, our study aims to analyse the incidence of variation of non-fusion ossification centre in the base of the odontoid and its anatomical structure characteristics, to compare ossification centre images and analyse the possible features of the ossification centre that can influence adult odontoid fractures.*

Materials and methods: *Fifty cases were selected for standard cervical CT of the normal axis bone (second cervical) anatomy to calculate the incidence of variation of the non-fusion ossification centre in the base of the odontoid and the indexes of associated anatomical structure. In addition, five dry bone samples with the odontoid were chosen for micro-CT to analyse the clear anatomic structure of the trabecular bone in the ossification centre.*

Results: *Incidence of variation of non-fusion ossification centre in the base of the odontoid was 28%. In the non-ossification group, the mean sagittal diameter of the base of odontoid (SDBO, mm) was 7.64 ± 1.29 mm, the mean transverse diameter of the base of odontoid (TDBO, mm) was 7.14 ± 1.55 mm, and the SDBO:TDBO ratio was 1.1 ± 0.22. In the ossification group, the mean SDBO was 7.7 ± 1.15 mm, the mean TDBO was 7.38 ± 1.32 mm, and the SDBO:TDBO ratio was 1.07 ± 0.21. There was no significant difference in the associated indexes between the ossification and non-ossification groups ($p > 0.05$). Micro-CT revealed the micro-structure of trabecular bone in the ossification centre and the close relationship between the trabecular bone and the odontoid. One existing non-ossification centre in the base of the odontoid was found in the five odontoid images. The trabecular bone indexes chosen in the target area of the ossification centre were weaker than those in other areas.*

Conclusions: *The variation rate of the non-fusion ossification centre in the base of the odontoid is relatively high and may be an important factor in the aetiology of type II and III odontoid fractures.* (Folia Morphol 2020; 79, 1: 141–147)

Key words: odontoid, ossification centre, trabecular bone, computed tomography, micro-computed tomography

Address for correspondence: Dr. S. Zhang, Human Anatomy Teaching and Research Section (Digital Medical Centre), Inner Mongolia Medical University Basic Medical College, Hohhot 010059, China, tel: +86 471 6657562, fax: +86 471 6657562, e-mail: cnshaojiezhang@126.com
Dr. Z. Li, Human Anatomy Teaching and Research Section (Digital Medical Centre), Inner Mongolia Medical University Basic Medical College, Hohhot 010059, China, tel: +86 471 6657551, fax: +86 471 6657551, e-mail: 13904717040@qq.com

#Wei Wang and Xing Wang contributed equally to this paper and share first authorship.
*Shaojie Zhang and Zhijun Li contributed equally to this paper and share correspondence.

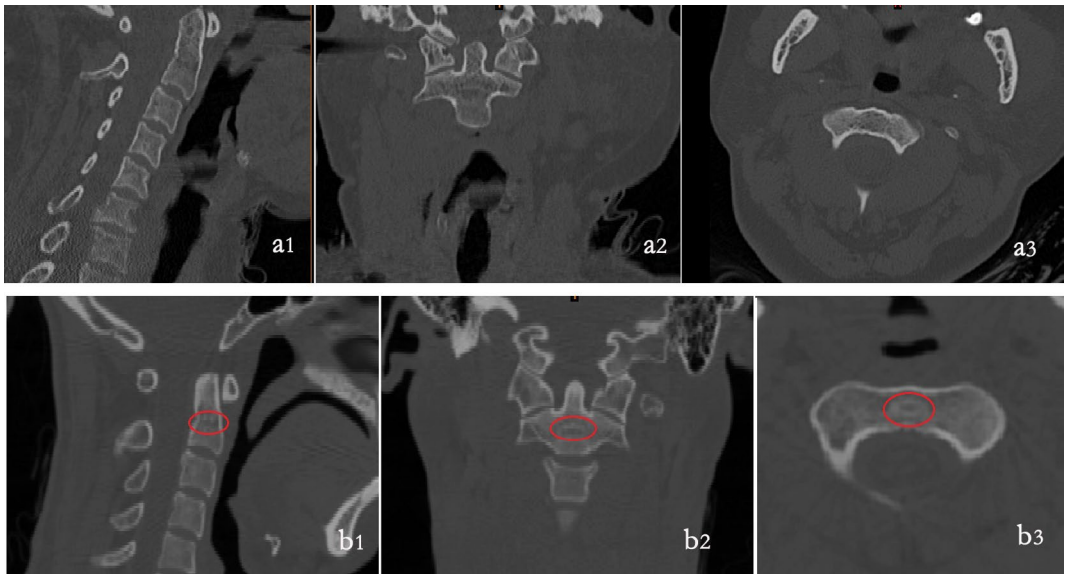

Figure 1. Computed tomography scan images of the normal adult odontoid. The red area shows there exits non-fusion ossification centre; **a1, b1.** Sagittal position; **a2, b2.** Coronal position, **a3, b3.** Horizontal position.

INTRODUCTION

The axis (C-2) is the second cervical vertebra. There are upwardly protruding finger-like protrusions on the vertebral body, which are called odontoid and it is associated segments behind the anterior arch of the atlas. The atlantoaxial ligament is composed of the cusp ligament, the pterygopalatine ligament and the transverse ligament of the atlas. The adult odontoid vegetative artery are basal artery and apical artery, which are anatomised and denser at the base. The axis is by far the most intricate of the upper vertebral bodies, and plays an integral role in atlantoaxial joint mobility, as well as stability of the cranio-cervical junction and upper cervical spine, while the odontoid is the central anatomical structure of upper cervical spine rotation, and its fracture can cause atlantoaxial instability characterised by occipital and posterior neck pain, especially with mild paraplegia and neuralgia, which contributes to difficulty in diagnosis and treatment [5, 10, 12, 19]. The incidence of odontoid fractures is high and this results from relatively complex influential factors and uncertain mechanisms. Type II odontoid fractures are the variety most frequently seen, and the special features of the anatomy of the odontoid may contribute to this finding [20]. The odontoid or dens develops from a primary mesenchymal ossification centre, and the epiphyseal plate of the ossification centre lies between the odontoid and the anterior body of the axis. Normally, the primary ossification centre of the odontoid will fuse with the axial anterior body around at 6 years of age. If the ossification centre fails to fuse, it can form a potential mechanically weak area, but the reason for non-fusion is still unclear [14]. Based on standard computed tomography (CT) and micro-computed tomography (micro-CT) scan images of the axis, the aim of our study is to analyse the incidence of variation of non-fusion ossification centre and its micro-CT imaging characteristics [16, 18, 21], and to provide evidence for accurate information about the relationship between the structure of the ossification centre and type II and III odontoid fractures, and its epidemiology.

MATERIALS AND METHODS

Standard CT data and scan indexes

We retrospectively analysed the CT scan images of the cervical spine with no odontoid structure variation in 50 consecutive patients who were selected for cervical CT scan of the normal central axis in the affiliated hospital from January to September 2018. In this cohort, there were 24 male and 26 female patients with ages ranging from 31 to 78 (mean age: 58) years. This type of study does not require formal consent of the patients (Fig. 1). The Z-axis flying focal spot technique was used to collect 64-row images using normal CT (Siemens CT, Siemens AG, Munich, Germany) with scan scope ranging from the skull base to the neck, scan index of 0.625 mm collimation value, and the following imaging parameters: slice thickness 0.75 mm, reconstruction interval 0.5 mm,

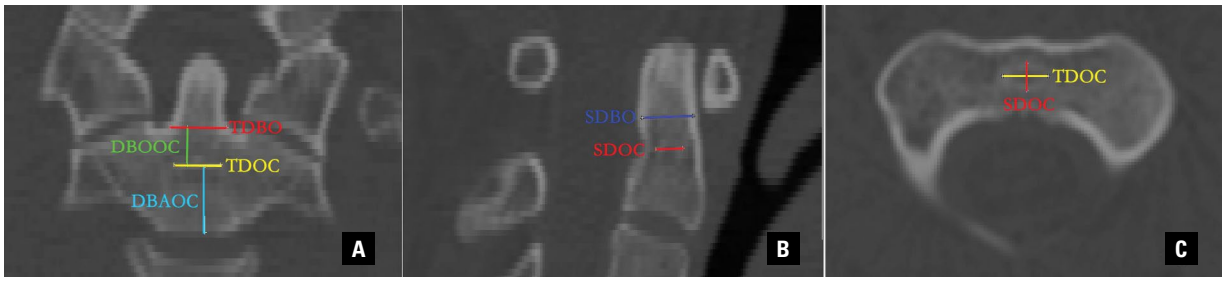

Figure 2. Computed tomography scan images of the measurement non-fusion ossification centre the indexes; **A.** TDBO, TDOC, DBOOC, DBAOC; **B.** SDBO, SDOC; **C.** TDOC, SDOC. Abbreviations — see text.

kilovolt A 140 kV, current 104 mA, kilovolt B 100 kV, and current 104 mA. The Digital Imaging and Communications in Medicine (DICOM)-data with lossless compression were used to store the CT images.

All the standard CT images were imported into the Mimics 16.0 software (Materialise, Belgium, Digital Medical centre of the Inner Mongolia University) to reconstruct the three-dimensional CT scan images for observation and measurement of the incidence of variation of non-fusion ossification centre and the following indexes:

— sagittal diameter of the base of odontoid (SDBO) (in the connection plane of the odontoid and the vertebral body);
— transverse diameter of the base of odontoid (TDBO);
— the transverse diameter of non-fusion ossification centre (TDOC, mm);
— the sagittal diameter of non-fusion ossification centre (SDOC, mm);
— the diameter of the base of odontoid and non-fusion ossification centre, (DBOOC, mm);
— the diameter of the bottom of the axis and non-fusion ossification centre (DBAOC, mm).

All the above indexes were selected and measured by three experienced CT radiologists using the bone age grading standard of CT based on Kellinghaus et al. [11], and each above index was measured twice to obtain a mean value, with data accuracy of 0.1 mm and permitted error range ± 0.1 mm (Fig. 2).

This study was conducted in accordance with the declaration of Helsinki. This study was conducted with approval from the Medical Ethics Committee of Inner Mongolia Medical University.

Micro-CT data, scan indexes and key rectification technique of imaging reconstruction

According to the anthropological skeleton identification standards, 5 dry bone samples with integral axial structure (provided by the Anatomy Teaching and Research Section of the Inner Mongolia Medical University) were chosen for the experiment.

After filtration and air correction of Micro-CT (Siemens Inveon MM PET/CT, Siemens AG, Munich, Germany), the bone samples were put on the objective table to perform a high-resolution scan and image collection using the optimal scan protocol (Siemens Inveon MM PET/CT Bin1 & High). Micro-CT was applied with the following unified setting indexes: voltage 40 kV, current 500 μA, and magnification on high-power mode.

Transverse images of samples were obtained with scan resolution ratio 40 μm, reconstruction interval 16.7 μm, slice thickness 16.7 μm, and scanning slice number 1024 pixels. The image data were imported into Inveon Research Workplace software workstation as DICOM data. Choosing all the trabecular bone in the ossification centre area of the transverse image as the target area, each index of bone trabecula was calculated by the built-in programme (MultiModal 3D visualisation) of the workstation.

The indexes that were measured in the non-fusion ossification group were: trabecular bone volume/ /total volume (BV/TV, %) that may decrease during osteoporosis, bone surface area/bone volume (BS/BV, mm^{-1}) that may decrease during bone formation increase, and bone trabecular thickness (Tb.Th, mm), which was the average thickness of trabecular bone, which may decrease during osteoporosis.

Statistical analysis

All data were recorded in Excel and data analysis was performed using SPSS 17.0 software. Descriptive results were expressed as mean ± standard deviation ($\bar{x} \pm s$). The non-paired samples were analysed by independent t test. The test level was set as $\alpha = 0.05$, and the threshold for statistical significance was set at $p < 0.05$.

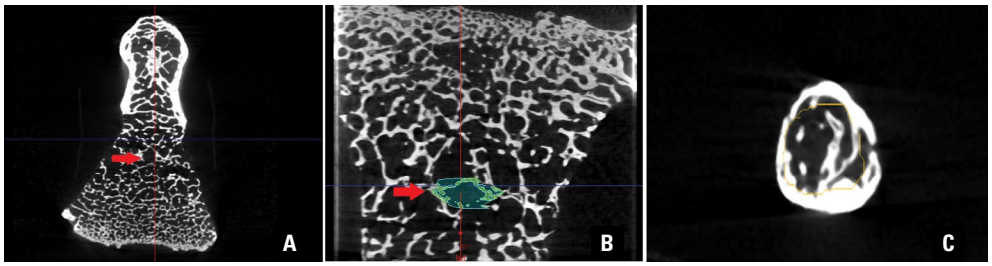

Figure 3. The micro-computed tomography images of the base odontoid; **A.** Ossification centre of coronal section (red arrow); **B.** Non-ossification centre of coronal section (red arrow, the green of region of interest); **C.** The three-dimensional image of non-fusion ossification centre.

RESULTS

Standard CT scanning

In 50 standard CT images of the odontoid, there were 14 cases of non-fusion ossification centre with incidence rate of 28%. In bone CT images, the base of the normal odontoid showed approximately the same density of cancellous bone, while the base of non-ossification odontoid showed significantly higher density of cancellous bone. The non-fusion ossification centre contained the cavities formed by absorbed trabecular bones (Fig. 1).

Micro-CT scanning

Through micro-CT scan, clear odontoid structure images were obtained, and one sample non-ossification centre in the base of the odontoid was found in each of the 5 odontoid images (Fig. 3).

The normal absorbed rod-shaped trabecular bone can form a complex mesh structure with the trabecular bone in other areas by transverse or oblique connection, which is distributed in the whole vertebral body. The trabecular bone of those CT images with non-fusion ossification centres showed high density and clear stratified images. The non-fusion ossification centre connected with other normal trabecular bones and the structure of the inner edge was very loose, containing low-density images of the partly absorbed trabecular bones or the cavities formed by absorbed trabecular bones. The trabecular bone indexes chosen in the target area of the non-fusion ossification centre were significantly weaker than those in the other areas of the vertebral body, combined with CT images, which indicated that the non-fusion ossification centre structure in the base of odontoid exist specialty [3, 17, 23].

Standard CT scanning measurement indexes

In the non-ossification group, the mean SDBO was 7.64 ± 1.29 mm, the mean TDBO was 7.14 ± ± 1.55 mm, and the SDBO:TDBO ratio was 1.1 ± 0.22. In the ossification group, the mean SDBO was 7.7 ± ± 1.15 mm, the mean TDBO was 7.38 ± 1.32 mm, and the SDBO:TDBO ratio was 1.07 ± 0.21. There was no significant difference between the two groups ($p > 0.05$; Table 1). In the non-ossification group, the mean SDOC was 5.34 ± 0.97 mm, the mean TDOC was 8.02 ± 1.64 mm, the mean DBOOC was 8.05 ± ± 1.57 mm, the mean DBAO was 11.85 ± 1.48 mm, and the ratio of SDOC:TDOC and DBCOC:DBAOC was 0.68 (Table 2).

Micro-CT scanning measurement indexes

Each index of the non-fusion ossification centre, fusion ossification centre and the odontoid trabecular bone was individually calculated by the built-in programme (MultiModal 3D visualisation) of the workstation. The measured indexes of the non-fusion ossification group were: BV/TV 0.287%, BS/BV 23.647 mm^{-1},

Table 1. The indexes comparison of the base of odontoid ($\bar{x} \pm s$, $n = 50$)

Groups	SDBO [mm]	TDBO [mm]	SDBO/TDBO
Non ossification	7.64 ± 1.29	7.14 ± 1.55	1.1 ± 0.22
Ossification*	7.7 ± 1.15	7.38 ± 1.32	1.07 ± 0.21

*Compared with non-ossification group: $p > 0.05$. Abbreviations — see text.

Table 2. The anatomic structure indexes of ossification centre ($\bar{x} \pm s$, $n = 14$)

	SDOC [mm]	TDOC [mm]	DBOOC [mm]	DBAOC [mm]	SDOC/TDOC	DBCOC/DBAOC
Non-fusion ossification group	5.34 ± 0.97	8.02 ± 1.64	8.05 ± 1.57	11.85 ± 1.48	0.68 ± 0.15	0.68 ± 0.12

Abbreviations — see text.

Table 3. The comparison of micro-computed tomography indexes in the base of odontoid ($\bar{x} \pm s$)

	BV/TV [%]	BS/BV [mm^{-1}]	Tb.Th [mm]
Non-fusion ossification centre	0.287	23.647	0.086
Fusion ossification centre	0.45 ± 0.05	12.33 ± 1.79	0.15 ± 0.02
Odontoid	0.60 ± 0.09	10.12 ± 1.33	0.22 ± 0.02

Abbreviations — see text.

Tb.Th 0.086 mm. The measured indexes of the fusion ossification group were: BV/TV 0.45 ± 0.05%, BS/BV 12.33 ± 1.79 mm^{-1}, Tb.Th 0.15 ± 0.02 mm. The measured indexes of the average of odontoid were: BV/TV 0.60 ± 0.09%, BS/BV 10.12 ± 1.33 mm^{-1}, Tb.Th 0.22 ± 0.02 mm (Table 3).

DISCUSSION

Odontoid fracture accounts for 9% to 15% of cervical spine injuries. Anderson and D'alonzo classification is one of the most important types of odontoid fractures. As introduced by Anderson et al. [1], odontoid fractures are classified into three groups, among which type II and type III odontoid fractures account for 95%. Type I fracture is an oblique fracture of the tip of the odontoid ligament. Type II fractures occur through the base of the odontoid, and type III fractures extend into the C-2 vertebral body. But the Anderson evaluation system [1] has obvious limitations; it cannot accurately distinguish between different types of odontoid fractures, if the fracture images are intermediate between the type II and the type III appearances. Subsequently, Grauer et al. [7, 15] proposed a modified new evaluation system for the Anderson type II odontoid fracture, which classified the type II fractures are those that are located between the inferior aspect of the anterior C1 ring and do not extend into the superior articular facets of C2. Fractures that are oblique in the anterior/posterior dimension may extend into the C2 vertebral body and still be considered type II fractures as long as there is no involvement of the superior C2 facets. If either of the superior C2 facets is involved, a fracture is considered a type III fracture. Aydin and Cokluk [2] researched the fusion of the cartilage ossification centre in the base of a child's odontoid based on magnetic resonance images. They found that the lower boundary of the odontoid is far lower than the plane connecting the highest point of the bilateral articular surface, and the real boundary lies in the neural part of the cartilaginous ossification centre in the base of the odontoid; this fact should be considered in the classification of odontoid fractures. However, the magnetic resonance images cannot clearly display the path of the trabecular bone in the ossification bone. With the development of a high-definition image technique, clearer micro-architecture images of the base of odontoid might be possible, and the definition and boundary of the base of the odontoid might be updated.

Through comparison of the standard CT images and the micro-CT images, we found that it is important to investigate the relationship between the non-fusion ossification centre and the type II and III odontoid fractures, because the variation rate of the non-fusion ossification centre in the base of odontoid is relatively high. Normally, the primary ossification centre of the odontoid will fuse with the axial anterior body around 6 years of age, which will fuse well with the vertebral body without remnants of the vestiges of the ossification centre. The trabecular bone formed by a normal absorbed ossification centre is homogeneous with that of the rest of the vertebral body, which shows medium-low images with a consistent CT value, and no anatomical weak area exists (Fig. 2A). In the presence of a non-fusion ossification centre, the clear structure can be displayed by the micro-CT images. Through comparison of trabecular bone indexes of the non-fusion ossification area, we found that the trabecular bone structure indexes of the non-fusion ossification centre were significant weaker than those of the other areas, which indicated that the anatomical structures of non-fusion ossification centres could be mechanically weaker than the normal trabecular bone of other parts (Fig. 2B).

The ossification centre lies in cancellous bone of the vertebral body of the axis, which connects with the lower edge of the odontoid, and if its location is lower than the plane connecting the highest point of the bilateral articular surface, it can be considered to be the lower edge of the base of odontoid. Hence, the type II odontoid fracture should be redefined as one at the junction of the odontoid and the neural part of axial vertebral body [4, 24]. Through observation and measurement of adult odontoid standard CT images, we found that the base of the normal odontoid is relatively wide. In view of this, we speculated that the larger the diameter of the base of the odontoid, the more stable the connection of the odontoid and axial

vertebral body, the smaller the percentage volume of the ossification centre in the odontoid and the vertebral body, the less the contribution of the ossification centre to development of basal fracture of the odontoid; the lower the location of ossification centre, the smaller the effect of the ossification centre on the base of the odontoid [6, 8, 9]. If the odontoid bears forces in any direction from the head, the energy can converge and transmit to the weakest trabecular bones of the inner ossification centre, which can cause precession avulsion of these areas, and the energy will transmit to the surrounding area along the avulsed trabecular bone; if the energy is relatively low, fractures of the base of odontoid will occur, which can form a type II odontoid fracture; if the energy is high enough, it can damage the unilateral or bilateral articular surface and result in a type III fracture [13] (type III odontoid fractures are fractures of the vertebral body of the axis involving the articular surface).

The reason for the failure of closure of the ossification centre of the odontoid process is unknown. It may be related to the influence of factors such as embryo development disorder, trauma, or infection. Further research should be targeted at working out how the micro-environment of bone might enhance pathways that promote cell differentiation, and the mechanisms by which this process is regulated [22].

CONCLUSIONS

The variation rate of the non-fusion ossification centre in the base of the odontoid is relatively high and may be the most important factor in the aetiology of type II and III odontoid fractures. More accurate studies are based on standard CT and micro-CT scans of large specimens of the axis (C-2) bone. Such studies are currently in progress.

Acknowledgements

This study was supported by Study on the Natural Science Foundation of China (81660358, 81260269, 81560348), the Inner Mongolia Medical University Science and Technology Million Project (YKD2015KJBW003, YKD2017KJBW(LH)062), Inner Mongolia Autonomous Region Health and Family Planning Commission Medical and Health Planning Research Project (201703015), Nature Science Foundation of Inner Mongolia Autonomous Region of China (2017MS(LH)0835, 2019MS08017), and Research Project Plan of Affiliated Hospital of Inner Mongolia Medical University (NYFY YB 004).

REFERENCES

1. Anderson LD, D'Alonzo RT, Anderson LD, et al. Fractures of the odontoid process of the axis. J Bone Joint Surg Am. 1974; 56(8): 1663–1674, indexed in Pubmed: 4434035.
2. Aydin K, Cokluk C. The segments and the inferior boundaries of the odontoid process of C2 based on the magnetic resonance imaging study. Turk Neurosurg. 2008; 18(1): 23–29, indexed in Pubmed: 18382973.
3. Boutroy S, Bouxsein ML, Munoz F, et al. In vivo assessment of trabecular bone microarchitecture by high-resolution peripheral quantitative computed tomography. J Clin Endocrinol Metab. 2005; 90(12): 6508–6515, doi: 10.1210/jc.2005-1258, indexed in Pubmed: 16189253.
4. Cho EJ, Kim SH, Kim WH, et al. Clinical results of odontoid fractures according to a modified, treatment-oriented classification. Korean J Spine. 2017; 14(2): 44–49, doi: 10.14245/kjs.2017.14.2.44, indexed in Pubmed: 28704908.
5. Colo D, Schlösser TPC, Oostenbroek HJ, et al. Complete remodeling after conservative treatment of a severely angulated odontoid fracture in a patient with osteogenesis imperfecta: a case report. Spine (Phila Pa 1976). 2015; 40(18): E1031–E1034, doi: 10.1097/BRS.0000000000000999, indexed in Pubmed: 26010035.
6. Graham RS, Oberlander EK, Stewart JE, et al. Validation and use of a finite element model of C-2 for determination of stress and fracture patterns of anterior odontoid loads. J Neurosurg. 2000; 93(1 Suppl): 117–125, doi: 10.3171/spi.2000.93.1.0117, indexed in Pubmed: 10879767.
7. Grauer JN, Shafi B, Hilibrand AS, et al. Proposal of a modified, treatment-oriented classification of odontoid fractures. Spine J. 2005; 5(2): 123–129, doi: 10.1016/j.spinee.2004.09.014, indexed in Pubmed: 15749611.
8. Jagannathan J, Dumont AS, Prevedello DM, et al. Cervical spine injuries in pediatric athletes: mechanisms and management. Neurosurg Focus. 2006; 21(4): E6, doi: 10.3171/foc.2006.21.4.7, indexed in Pubmed: 17112196.
9. Julien TP, Schoenfeld AJ, Barlow B, et al. Subchondral cysts of the atlantoaxial joint: a risk factor for odontoid fractures in the elderly. Spine J. 2009; 9(10): e1–e4, doi: 10.1016/j.spinee.2009.04.025, indexed in Pubmed: 19535297.
10. Kandziora F, Chapman JR, Vaccaro AR, et al. Atlas fractures and atlas osteosynthesis: a comprehensive narrative review. J Orthop Trauma. 2017; 31 Suppl 4: S81–S89, doi: 10.1097/BOT.0000000000000942, indexed in Pubmed: 28816879.
11. Kellinghaus M, Schulz R, Vieth V, et al. Forensic age estimation in living subjects based on the ossification status of the medial clavicular epiphysis as revealed by thin-slice multidetector computed tomography. Int J Legal Med. 2010; 124(2): 149–154, doi: 10.1007/s00414-009-0398-8, indexed in Pubmed: 20013127.
12. Megan EG, Michael PK. Fractures of the axis: a review of pediatric, adult, and geriatric injuries. Curr Rev Musculoskelet Med. 2016; 9(4): 505–512, doi: 10.1007/s12178-016-9368-1, indexed in Pubmed: 27686572.
13. Niemeier TE, Dyas AR, Manoharan SR, et al. Type III odontoid fractures: A subgroup analysis of complex, high-energy fractures treated with external immobilization. J Craniovertebr Junction Spine. 2018; 9(1): 63–67, doi: 10.4103/jcvjs.JCVJS_152_17, indexed in Pubmed: 29755239.

14. O'Brien WT, Shen P, Lee P. The Dens: normal development, developmental variants and anomalies, and traumatic injuries. J Clin Imaging Sci. 2015; 5: 38, doi: 10.4103/2156-7514.159565, indexed in Pubmed: 26199787.
15. Ouyang PR, He XJ, Cai X. [Classification of upper cervical fractures: a review]. Zhongguo Gu Shang. 2017; 30(9): 872–875, doi: 10.3969/j.issn.1003-0034.2017.09.018, indexed in Pubmed: 29455493.
16. Perilli E, Parkinson IH, Reynolds KJ. Micro-CT examination of human bone: from biopsies towards the entire organ. Ann Ist Super Sanita. 2012; 48(1): 75–82, doi: 10.4415/ANN_12_01_13, indexed in Pubmed: 22456020.
17. Peyrin F. Evaluation of bone scaffolds by micro-CT. Osteoporos Int. 2011; 22(6): 2043–2048, doi: 10.1007/s00198-011-1609-y, indexed in Pubmed: 21523402.
18. Ritman EL. Current status of developments and applications of micro-CT. Annu Rev Biomed Eng. 2011; 13: 531–552, doi: 10.1146/annurev-bioeng-071910-124717, indexed in Pubmed: 21756145.
19. Ryan MD, Henderson JJ. The epidemiology of fractures and fracture-dislocations of the cervical spine. Injury. 1992; 23(1): 38–40, doi: 10.1016/0020-1383(92)90123-a, indexed in Pubmed: 1541497.
20. Smith HE, Kerr SM, Fehlings MG, et al. Trends in epidemiology and management of type II odontoid fractures: 20-year experience at a model system spine injury tertiary referral center. J Spinal Disord Tech. 2010; 23(8): 501–505, doi: 10.1097/BSD.0b013e3181cc43c7, indexed in Pubmed: 20940632.
21. Sung MJ, Kim KT, Hwang JH, et al. Safe Margin beyond Dens Tips to Ventral Dura in Anterior Odontoid Screw Fixation : Analysis of Three-Dimensional Computed Tomography Scan of Odontoid Process. J Korean Neurosurg Soc. 2018; 61(4): 503–508, doi: 10.3340/jkns.2018.0034, indexed in Pubmed: 29991109.
22. Tang XM, Liu C, Huang K, et al. [Analysis of a three-dimensional finite element model of atlas and axis complex fracture]. Zhonghua Yi Xue Za Zhi. 2018; 98(19): 1484–1488, doi: 10.3760/cma.j.issn.0376-2491.2018.19.006, indexed in Pubmed: 29804415.
23. Tassani S, Perilli E. On local micro-architecture analysis of trabecular bone in three dimensions. Int Orthop. 2013; 37(8): 1645–1646, doi: 10.1007/s00264-013-1989-z, indexed in Pubmed: 23835557.
24. Watanabe M, Sakai D, Yamamoto Y, et al. Analysis of predisposing factors in elderly people with type II odontoid fracture. Spine J. 2014; 14(6): 861–866, doi: 10.1016/j.spinee.2013.07.434, indexed in Pubmed: 24055610.